

Ionic Strength and Curvature Effects in Flat and Highly Curved Polyelectrolyte Brushes

R. Hariharan,^{†,‡} C. Biver,[§] J. Mays,^{||} and W. B. Russel^{*,†}

Department of Chemical Engineering, Princeton University, Princeton, New Jersey 08544, Elf Atochem, 95 Rue Danton, BP 108, 92300 Levallois-Perret, France, and Department of Chemistry, University of Alabama, Birmingham, Alabama 35294-1240

Received December 15, 1997; Revised Manuscript Received June 19, 1998

ABSTRACT: Adsorption of poly(*tert*-butylstyrene)/poly(styrenesulfonate) diblocks on polystyrene latices from water is reported and interpreted with scaling theories to demonstrate the effects of ionic strength and curvature on layer thickness. The adsorbed amount increases with ionic strength from no added salt to 0.1 M, forming a dense polyelectrolyte brush. The influence of particle radius on layer thickness is correlated quantitatively via the Daoud–Cotton model, but the effect on surface coverage is obscured by uncontrolled aspects of surface chemistry. Decreasing the ionic strength dramatically increases the dimensions of polyelectrolyte micelles and adsorbed layers; the sensitivity, while strongly coupled with curvature, is overestimated by all existing theories. A simple scaling theory that accounts for electrostatic excluded volume more appropriately captures the trends qualitatively.

1. Introduction

Adsorption of diblock polymers at solid–liquid interfaces has been a subject of both theoretical^{1,2} and experimental interest.^{3–6} Although neutral diblocks have been investigated and reviewed in detail,^{7–9} attention on polyelectrolyte diblocks is relatively recent. In addition to the entropic and excluded volume interactions for a neutral polymer, intra- and interchain repulsions due to the charges along the backbone contribute to the overall free energy for polyelectrolytes. Despite the complexity posed by the nonlinearity of the Poisson–Boltzmann equation, these factors have been captured relatively well for polyelectrolytes in the bulk.^{10,11} At solid–liquid interfaces, however, even the recent attention has stimulated few experiments with well-characterized polyelectrolyte brushes on colloidal spheres. Changing from a flat surface to a curved particle decreases the excluded volume interactions in a dense layer as the volume occupied per chain increases with distance from the surface. For a fixed chain density, the energy penalty for excluded volume interactions is stiffer for a surface of lower curvature, so one would expect the surface coverage to decrease with increasing particle radius. If the surface density is held fixed, the chains on a flatter surface interact more strongly with neighbors, causing the layer to swell. Thus, one would expect the layer thickness to increase with particle radius.

The objective of this paper is to present experimental evidence, complemented by simple models, to demonstrate several effects of curvature and ionic strength on polyelectrolyte brushes:

(1) Adsorption of a polyelectrolyte from a polar solvent onto colloidal particles: Extension of studies on macroscopic mica¹² and silica¹³ surfaces to colloidal particles

is nontrivial. Polyelectrolytes tend not to adsorb onto a surface of like charge at low to moderate ionic strength, while hydrophobic colloidal particles can flocculate even at modest salt concentrations. Hence a large increase in salt concentration will drive adsorption but also promotes flocculation. The correct procedure for obtaining individually dispersed, coated colloidal particles depends on system parameters such as surface hydrophobicity, particle size, block composition, and solvent quality.

(2) Influence of curvature on surface coverage and layer thickness: We aim to connect experiments on macroscopic surfaces to colloidal dispersions by quantifying surface coverage and layer thickness as functions of particle size and correlating the behavior through the spherical blob model of Daoud and Cotton,¹⁴ as initiated in our previous paper.¹⁵

(3) Influence of ionic strength on polymer dimensions in micelles and coated particles: We wish to measure the effect over a broad range of ionic strengths and compare the data and that in the literature against theories for polyelectrolyte brushes. Any discrepancies that emerge will motivate further development of the theory.

This paper begins with a brief review of theoretical and experimental developments relevant to polyelectrolyte brushes and curvature in neutral brushes. Section 3 then describes our measurements of adsorption of narrow distribution poly(*tert*-butylstyrene)/poly(styrenesulfonate) chains onto well-characterized polystyrene latex particles and the dimension and aggregation number of the micelles in bulk. Section 4 analyzes the surface coverage and layer thickness in the light of existing theories, explaining the applicability of the Daoud–Cotton model¹⁴ and the limitations of theories for polyelectrolyte brushes. We overcome the latter in section 5 through a simple scaling model for the effect of ionic strength in the limits of flat and highly curved surfaces. Section 6 summarizes the work.

* Author to whom all correspondences should be addressed.

[†] Princeton University.

[‡] Current address: Polymer Materials Laboratory, General Electric CR&D, Schenectady, NY 12301.

[§] Elf Atochem.

^{||} University of Alabama.

2. Background

2.1. Effect of Curvature. Curvature was addressed previously^{15,16} through the Daoud–Cotton model, originally proposed for star polymers and recognized by Marques et al.¹ and Halperin¹⁷ as appropriate for star polymers, micelles, and coated spherical particles. The model for a p -arm star polymer¹⁴ assumes a close packed assembly of blobs emanating from the core and equates the surface area at any radius r with the cross sectional area of a blob of diameter ξ times the number of arms

$$p\xi^2(r) = 4\pi r^2 \quad (1)$$

For chains attached to a sphere of radius R the blob size varies linearly with radial distance:

$$\xi \approx \frac{r}{R\sqrt{\sigma}} \quad (2)$$

where the chain density $\sigma = \Gamma N_a/M$ follows from Γ , the mass adsorbed per unit area; N_a , Avagadro's number; and M , the total molecular weight. The number of segments in a blob (N_ξ) is related to the blob size in good solvents through

$$\frac{\xi}{l_k} \approx N_\xi^{3/5} \left(\frac{v}{l_k^3} \right)^{1/5} \quad (3)$$

where l_k is the statistical segment or Kuhn length and v is the binary cluster integral characterizing the polymer–solvent interaction. Setting the integral of the segment density equal to the total number of segments within the brush relates the layer thickness L to the particle radius as

$$\left(\frac{L}{R} + 1 \right)^{5/3} = 1 + \frac{kL_c}{R} \left(\frac{v\sigma}{l_k} \right)^{1/3} \quad (4)$$

where the constant k is close to unity and L_c is the contour length of the chains.

The Marques–Joanny theory^{1,2} for adsorption onto flat surfaces was extended by Ligoure and Leibler¹⁸ to end-functionalized polymer on spherical surfaces. Terms accounting for the adsorption energy of the end segment and the translational entropy of chains in the adsorbed layer were balanced against the elastic and excluded volume interactions from the Daoud and Cotton model. The resulting equilibrium surface coverage for typical values of the molecular parameters decreases monotonically with increasing particle size. An analogous analysis by Qiu and Wang¹⁹ adopted the Daoud–Cotton model for both polymeric micelles and particles with adsorbed diblock copolymer. By minimizing the free energy, they distinguish regimes where micellization or adsorption are favored as a function of block and particle sizes, concluding that the polymer chains have a greater tendency to stay in micelles with increasing particle size, consistent with the Ligoure–Leibler result.

The first experimental work probing the influence of curvature dealt with poly(vinyl alcohol) adsorption on polystyrene latex particles, first concluding that the volume occupied by an adsorbed chain remains as in bulk solution²⁰ and then arguing that the surface coverage should be independent of particle radius.²¹ This implies that the ratio of the volume of the adsorbed layer to the particle surface area is independent of particle size, meaning that L increases with increasing R . Later

work on adsorption of pluronic triblock (PEO–PPO–PEO) copolymers on polystyrene latices of five particle sizes seemed to contradict the above notion^{22,23} for triblocks with short midblocks and longer tails. Instead, the measured surface coverage increased systematically with increasing particle size, though a more symmetrical triblock suggested an opposite but less pronounced trend.

Singh et al.²⁴ addressed curvature through adsorption of end-functionalized polystyrene from toluene on model rough surfaces created by spin coating colloidal silica beads of varying sizes on silicon substrates. They observed a maximum in the adsorbed amount as a function of curvature, because the adsorbed chains on one sphere can interfere with those on the adjacent sphere when the sphere radius is comparable to the layer thickness ($L/R \sim 1$). For larger radii ($L/R < 0.1$), hindrance is unimportant and the surface coverage decreases monotonically with increasing radius, reaching a plateau for $L/R \sim 0.01$ where curvature apparently becomes unimportant. The trend is in quantitative agreement with the theory of Ligoure and Leibler.¹⁸

Merrington et al.²⁵ also adsorbed end-functionalized polystyrene from toluene on monodisperse silica particles of diameters ranging from 101 to 760 nm. Surface coverage measured by thermal gravimetry yielded no systematic trend as a function of particle size. Layer thicknesses were not measured, but calculations of the radius of gyration indicate $0.01 < L/R < 0.09$. On the basis of the above studies, no clear conclusion emerges regarding the influence of curvature on adsorbed amount.

2.2. Polyelectrolyte Brushes. Theoretical Advances. Miklavic and Marcelja²⁶ and Misra et al.²⁷ extended the self-consistent Milner–Witten–Cates theory²⁸ to tethered polyelectrolytes to predict a roughly parabolic segment density profile that extends further with increasing charge density or decreasing salt concentration. For low ionic strengths, the dependence of the brush height on the graft density deviates significantly from the scaling for uncharged brushes ($\sigma^{1/3}$).²⁹ In response, blob models^{30–32} have been formulated in seeking analytical representations of the trends predicted by the self-consistent field theory. In the limit as $R \rightarrow \infty$ of eq 4 these take the form

$$L \sim L_c \left(\frac{v\sigma}{l_k} \right)^{1/3} \quad (5)$$

and offer different approximations for the excluded volume parameter v and the Kuhn length l_k .

Motivated by earlier work on semidilute solutions,³¹ Pincus³⁰ ignores chain stiffening such that $l_k = l$, with l the Kuhn length for an equivalent uncharged chain, and expresses the electrostatic contribution in terms of the osmotic pressure, which translates into

$$v \sim \frac{l}{\kappa^2} \quad (6)$$

when the added salt concentration dominates the counterions. κ^2 is related to the salt concentration C_s via $8\pi l_b C_s N_a$ with the Bjerrum length $l_b = 0.714$ nm. v corresponds to the effective volume of a charged rod of length l and radius $1/\kappa$, which is argued to represent the excluded volume in highly crowded solutions. The layer thickness from eq 5 then varies with ionic strength as $L \sim C_s^{-1/3}$. When the added salt concentration falls below the concentration of counterions in the brush, $N\sigma/l$

L , with N the number of segments per chain, the swelling of the layer reaches an asymptote independent of C_s and σ .

Zhulina et al.³³ developed an analytical theory describing the structure of both unsalted and salted polyelectrolyte brushes. The free energy functional is expressed as a sum of entropy and excluded volume, incorporating both nonelectrostatic and electrostatic interactions. The Debye–Hückel approximation accounts for repulsions between fixed charges on the chain. For the unsalted brush, the electrostatics is shown to dominate the nonelectrostatic excluded volume interactions, via the insensitivity of the brush height with changing temperature. For the salted brush, in the regime where added salt concentration far exceeds the counterion concentration, they predict

$$L \sim L_c \sigma^{1/3} C_s^{-1/3} \quad (7)$$

consistent with the Pincus prediction.

Argiller and Tirrell³² instead adopted Fixman's¹¹ treatment of local chain stiffening with $l_k \sim 1/l_b \kappa^2$ and approximated the excluded volume as $v \sim l_k^3$, which treats the segments as spheres of diameter l_k . The resulting layer thickness varies with salt concentration as $L \sim C_s^{-2/3}$. Dan and Tirrell³⁴ extended this treatment to charged brushes on spheres through the Daoud–Cotton model.

Alternatively, one could adopt a scaling form of the electrostatic wormlike chain theory developed by Odijk, Fixman, and co-workers for polyelectrolytes in dilute solution.^{10,11,35} This models a Kuhn segment as a charged cylinder of length $l_k \sim 1/l_b \kappa^2$, such that $l_k \kappa > 1$. The electrostatic excluded volume between cylindrical segments of such high aspect ratio is $v \sim l_k^2 \kappa^{-1}$, which leads to $L \sim C_s^{-1/2}$.

von Goeler and Muthukumar³⁶ simulate tethered chains by enumerating configurations and then calculating and minimizing the free energy associated with chain stretching and screened Coulombic interactions between point charges described through the linearized Poisson–Boltzmann equation. Various regimes are delineated by values of the dimensionless parameters $\kappa \sqrt{Nl}$ and $v_e N^{5/2}$. Strong stretching emerges when

$$v_e N^{5/2} = \frac{2\pi\sigma L_c^2 N^{1/2} l}{l_b} \quad (8)$$

the electrostatic energy between two charged Gaussian coils tethered $\sigma^{-1/2}$ apart, is much greater than $N l_b \kappa^2$, the square of the ratio of the coil dimension to the Debye length. Then $L \sim L_c (\sigma l_b \kappa^2)^{1/3} \sim C_s^{-1/3}$. The sensitivity decreases with decreasing $v_e N^{5/2}$ but no other well-defined regime is evident. Since the Debye length κ^{-1} is treated as a constant, the predictions remain valid only when counterions are negligible, i.e., not for large $v_e N^{5/2}$ and low $N^{1/2} l_k$.

Table 1 summarizes the salient features of the existing theories. While Pincus ignores local chain stiffening entirely, Tirrell and coworkers^{32,34} employ an electrostatic Kuhn length in accord with Fixman.¹¹ Pincus and Argiller and Tirrell treat the excluded volume as a function of ionic strength, but differently from each other and the electrostatic wormlike chain theory. The others implicitly account for both local chain stiffening

Table 1. Analyses of Polyelectrolyte Brushes Based on Monte Carlo Simulations (MC), Mean Field (MF), and Self-Consistent Field (SCF) Theories

ref	method	κ^2	l_k	v
Pincus ³⁰	MF	$C_s + (N\sigma/2N_a L)$	1	l/κ^2
Argiller and Tirrell ³²	MF	$C_s + (N\sigma/2N_a L)$	$1/l_b \kappa^2$	l_k^3
Miklavic and Marcelja, ²⁶ Misra et al. ²⁷	SCF	C_s		linearized PB eq
von Goeler and Muthukumar ³⁶	MC	C_s		linearized PB eq
Zhulina et al. ³³	SCF	$C_s + (N\sigma/2N_a L)$		linearized PB eq

and excluded volume, but rather crudely, in employing the linearized Poisson–Boltzmann equation with point charges.

Experimental Findings. Although the adsorption of polyelectrolyte homopolymers has been investigated in detail,⁹ adsorption of amphiphilic polyelectrolytes is still rare. Pefferkorn et al.³⁷ created adsorbed layers of poly(2-vinylpyridine)/poly(styrenesulfonate) on silica by two approaches. In the first, poly(2-vinylpyridine)/poly(styrene) was adsorbed from an organic solvent and then sulfonated in the heterogeneous media. In the second, poly(2-vinylpyridine)/poly(styrenesulfonate) was adsorbed from an aqueous solution of 0.05 M NaCl at pH 8. They found the latter to be more stable.

We have realized nearly monodisperse, well-defined poly(*tert*-butylstyrene)/poly(styrenesulfonate) diblocks by sulfonation of a poly(*tert*-butylstyrene)/poly(styrene) diblock synthesized by anionic polymerization.³⁸ With these polymers, Guenoun et al.³⁹ observed the formation of polymeric micelles with an undetectably low critical micelle concentration and measured the aggregation number and size with small angle neutron and light scattering. Increasing salt concentration collapses the micellar structure from highly extended to relatively compact aggregates, though with a weaker dependence on salt concentration than expected from theories for flat plates.^{30,34} The aggregation number proved independent of the salt concentration from 10^{-4} to 10^{-2} M, but decreased to about half at high salt (0.1 to 0.5 M). Watanabe et al.¹² obtained full coverage for two molecular weights on mica and found the range of interaction more sensitive to added salt than micellar dimensions,³⁹ but still weaker than the theoretical predictions. High coverages were also obtained¹³ on a SiO₂ surface from a 1 M salt solution. The adsorbed amounts for the two molecular weights were consistent with the scaling relation of Dan and Tirrell,³⁴ $\sigma \sim N_{PSS}^{-6/5}$, for the dependence on the number of segments N_{PSS} in the soluble block.

Using SANS, Mir et al.⁴⁰ obtained segment density profiles of polyelectrolyte brushes of “medium” and “high” (Md and Hd) grafting densities in pure water as well as salt solutions. In pure water, the density profile is rather gently sloped, extending far from the surface, consistent with the predictions of Zhulina et al.³³ However, the layer thickness was found to be a weak function of the graft density contrary to the predictions of Pincus³⁰ and Zhulina et al.³³ The scaling exponent however is not readily available because the first moment of the segment density (the calculated layer thickness) has not been presented as a function of salt concentration. For the salted brushes, the Md brushes are found to be much more sensitive to salt concentration changes than the Hd brushes. This opposes the von Goeler and Muthukumar³⁶ prediction which suggests that brushes with higher surface coverages (higher

Table 2. Particle Characterization

2R (nm)	polydispersity (%)	area per sulfate, nm ²
91	10.7	21
137	2.3	20
202	4.6	14
301	2.0	10

Table 3. Molecular Characterization of Diblock Copolymer (MT3)

$M_A = 4.31$ kg/mol
$M_B = 145.7$ kg/mol
$M_w/M_n = 1.04$
Fraction of charged monomers = $f = 0.87$

v_c) will shrink more readily upon addition of salt.

Guenoun et al.⁴¹ employed X-ray reflectivity to probe the structure of a free-standing black film drawn from a diblock polyelectrolyte solution. The thickness of the film estimated using a model of a single homogeneous slab is found to be insensitive to the salt concentration at ionic strengths below 10^{-2} M. Above 0.2 M a steady drop in the layer thickness is found to follow the scaling relationship $L \sim C_s^{-0.31}$, in close agreement with the value predicted by Pincus. However, it is not clear if the surface coverage in these experiments is indeed constant with changing ionic strength, as would be required for an appropriate comparison against the theory.

3. Experimental Section

3.1. Materials. Low polydispersity polystyrene particles (Interfacial Dynamics Corp., Portland, OR) with reported mean diameters from TEM of $2R = 91, 137, 202$, and 301 nm (Table 2) were used without further cleaning in the adsorption experiments. The large area per sulfate group on the surface implies extended hydrophobic (polystyrene) regions with isolated or clustered charge groups.

The poly(*tert*-butylstyrene)/sodium poly(styrenesulfonate) for this study (MT3) has a total molecular mass of 150 kg/mol (Table 3). Polymer solutions in doubly distilled water were equilibrated for a few days and filtered through a $0.6 \mu\text{m}$ polycarbonate filter (Costar Corp., Cambridge, MA). Salt solutions prepared from sodium chloride (Fluka Chemika-Biochemika, Ronkonkoma, NY) were filtered through a $0.1 \mu\text{m}$ poly(vinylidene fluoride) membrane (Millipore Inc., Bedford, MA).

3.2. Procedure. A 3000 ppm polymer solution was prepared by adding polymer powder grain by grain to a flask containing continuously stirred, doubly distilled, deionized water. In the adsorption experiments, the initial polymer concentration of around 2000 ppm was chosen to provide 4 times the polymer required for a surface coverage of 4 mg/m^2 . The concentration of particles in all adsorptions is small to make particle–particle interactions unimportant.

Since Amiel et al.¹³ and Watanabe et al.¹² only succeeded in adsorbing this polymer at high salt concentrations, we initially attempted 0.1 M NaCl but found the bare particles to be unstable. Fortunately, partial coverage is obtained on polystyrene even without added salt, presumably due to a higher surface hydrophobicity than for mica, and served to stabilize the particles polymerically before exposure to high salt conditions. Hence adsorption was performed sequentially with partial coverage obtained by mixing the polystyrene dispersion with the polymer solution, waiting for 4–5 h, and then adding 1 M NaCl solution to achieve a final ionic strength of 0.1 M. For one of the particle sizes (137 nm) we also performed the first adsorption at 0.025 M NaCl at which the bare particles are stable, prior to increasing the salt concentration to 0.1 M. We verified that the adsorbed amount attains a plateau at the initial concentration of 2000 ppm, by adsorbing at concentrations of 1200 ppm and 2800 ppm with the same particle concentration.

The depletion method for determining surface coverage⁸ involves measuring the polymer concentration in the supernatant solution after centrifuging to remove the colloidal particles. The separation proved difficult, however, because of the small density difference between the particles ($\rho_1 = 1055 \text{ kg/m}^3$) and the water, hindrance by the back-flow of water⁴² at moderate volume fractions of the particles and micelles, and increased hydrodynamic drag on the particles due to the adsorbed polymer. We, therefore, diluted the system with fresh 0.1 M NaCl solution in a ratio of 1:5 and employed a high-speed centrifuge (Sorvall Instruments, Wilmington, DE) with a tilted rotor (SS-34, rotor angle = 34°) and transparent polycarbonate tubes at 20000g. Since the micelles also settle, reducing the measured concentration below the actual supernatant concentration, we calibrated with polymer solutions (no particles) at 0.1 M ionic strength and initial concentrations from 200 to 400 ppm¹⁶ to correct for polymer lost from the supernatant. Then the surface coverage Γ follows from a mass balance in which we assume free polymer to be excluded from the sediment. To minimize the error associated with that assumption, the experiments were designed with a small sediment volume, reducing the uncertainty in the surface coverage to less than 0.25%.

Dynamic light scattering determines the hydrodynamic size of the diblock copolymer micelles and the hydrodynamic thickness of the adsorbed layer on particles from measurements of the diffusion coefficient D_0 , which for a Brownian sphere of hydrodynamic radius R follows the Stokes–Einstein relationship⁴³

$$D_0 = \frac{kT}{6\pi\mu R} \quad (9)$$

with μ the viscosity of the solvent and T the absolute temperature. The difference between the hydrodynamic radii of coated and bare particles is defined⁴⁴ as the hydrodynamic layer thickness and assumed to equal L . The polydispersity characterized via $(\bar{R}^2 - \bar{R}^2)/\bar{R}^2$ is extracted from the quadratic term in the second moment fit of the intensity autocorrelation function.

Our experiments employed a light scattering goniometer and BI-2030AT digital correlator (Brookhaven Instruments Corp., Holtsville, NY) along with a He–Ne laser (Lexel Corp., Palo Alto, CA) at a wavelength of $\lambda = 514.5 \text{ nm}$ and a scattering angle typically of 90° . Filtering the solvent suffices to remove dust before static and dynamic light scattering measurements. The TEM diameters in Table 2 were taken as the bare hydrodynamic size, since flocculation prevented dynamic light scattering at 0.1 M NaCl and measurements at 0.05 M NaCl yielded only a 3 nm larger diameter for the 137 nm particles.

Static light scattering determines the molecular weight of a micelle and hence the aggregation number p in dilute solutions. Knowledge of the poly(*tert*-butylstyrene) block bulk density (950 kg/m^3) and molecular mass M_{PBS} then determines the radius of the micellar core, which sets the chain density σ . With this, one can compare the micelles to other surfaces of known σ . The excess scattering $I(q)$ from a dilute micellar solution depends on the concentration C_p and the wave number q through the Rayleigh ratio⁴⁵

$$\frac{KC_p}{I(q)} = \frac{1}{pM} \left[1 + \frac{q^2 R_g^2}{3} + O(qR_g)^3 \right] \quad (10)$$

where p and R_g are the aggregation number and radius of gyration of the micelle and M is the molecular mass of each diblock. The constant K accounts for the geometry through the scattering volume V and the distance r to the detector, and solution properties such as the refractive index increment from the polymer¹³ (dn/dc_p) = $1.68 \times 10^{-4} \text{ m}^3/\text{kg}$ as

$$K = \frac{2\pi^2 n_0^2}{\lambda^4 N_A} \left(\frac{dn}{dc_p} \right)^2 \frac{I_0 V}{r^2} \quad (11)$$

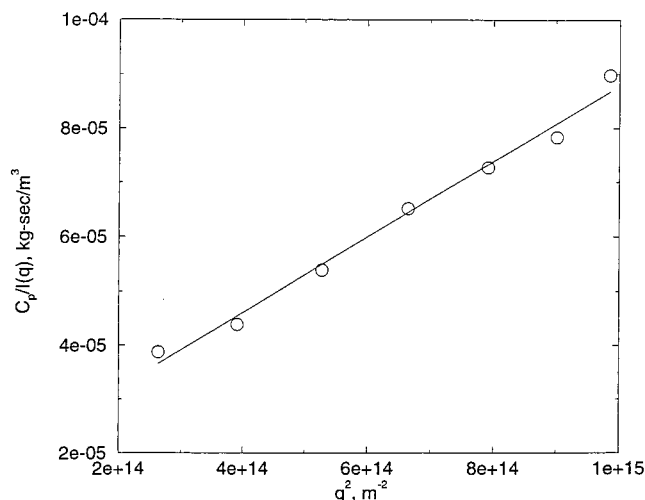


Figure 1. Static light scattering intensities for MT3 at 100–300 ppm.

where n_0 is the refractive index of water and I_0 is the intensity of the incident light. Calibration with benzene, for which the reported Rayleigh ratio is $r^2 I(90^\circ)/VI_0 = 2.1 \times 10^{-7}/\text{m}$, determines V/r^2 . Then for the dilute micellar solutions eq 10 suggests that plotting $KC_p/I(q)$ versus q^2 should yield a straight line with a slope of $R_g^2/(3pM)$ and an intercept of $1/pM$.

Measurements at 100–300 ppm, over an angular range of $30^\circ \leq \theta \leq 150^\circ$ for filtered polymer solutions of MT3 in doubly distilled, deionized water are extrapolated to $C_p \rightarrow 0$ and plotted versus the square of the wavenumber in Figure 1. The best-fit straight line yields a radius of gyration $R_g = 102 \pm 6$ nm and a micellar molecular mass of $(3.4 \pm 0.6) \times 10^3$ kg/mol. The single chain molecular mass then indicates an aggregation number of $p = 23 \pm 4$, in excellent agreement with the value of 22 from recent neutron scattering experiments on the same system.^{1,2}

Guenoun et al.^{39,46} reported an aggregation number of $p = 38$ for micelles of a lower molecular mass diblock MT2 ($M_{\text{PSS}} = 83$ kg/mol, $M_{\text{PtBS}} = 4.2$ kg/mol, 89% sulfonated) at similar ionic strengths. Wittmer and Joanny⁴⁷ predict the aggregation number for polyelectrolyte diblocks to obey the scaling

$$p \sim \frac{M_{\text{PtBS}}^{2/3}}{M_{\text{PSS}}} \quad (12)$$

in deionized water. With the data for MT2, the Wittmer and Joanny scaling predicts an aggregation number of 22 for MT3, which is within 5% of the measured value. Therefore, we assume this scaling to provide a reasonable estimate for the aggregation number at finite salt concentrations as well.

4. Results and Discussion

4.1. Effect of Curvature. Adsorption with no added salt yields $\Gamma = 0.05 \pm 0.02$ mg/m², corresponding to a very sparsely covered surface with roughly 70 nm between adsorbed chains. The significant uncertainty arises from the small difference between the initial and final concentrations in the supernatant. The low adsorbed amount implies that the energy of adsorbing poly(*tert*-butylstyrene) on the hydrophobic surface is balanced by long range electrostatic repulsions between the poly(styrenesulfonate) blocks. Nonetheless, this adsorption suffices to stabilize the dispersion at high ionic strengths.

Increasing the salt concentration to 0.1 M NaCl screens the backbone charges and lessens the electrostatic penalty for adsorption of additional chains, yielding a dramatic rise in surface coverage (Table 4) for all four particle sizes. Measurements 9 days after adsorp-

Table 4. Equilibrium Plateau Surface Coverage and Layer Thickness at 0.1 M NaCl as a Function of Particle Size

particle diameter, nm	surface coverage, mg/m ²	layer thickness, nm
91	2.2	74
137	1.9	61
202	4.2	110
301	3.4	104

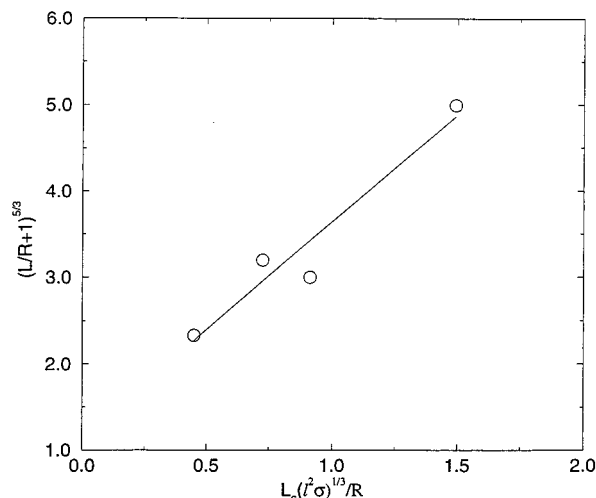


Figure 2. Data for MT3 adsorbed on polystyrene latices plotted according to the Daoud–Cotton theory. A best-fit straight line yields an intercept of 1.16.

tion equaled those after 32 days within experimental error. The same result was obtained by a two-step process, with adsorption first at 0.025 M and then at 0.1 M, and for different bulk copolymer concentrations ($750 \text{ ppm} < C_p < 2100 \text{ ppm}$ for the 137 nm particles). These observations imply that the data in Table 4 represent the full equilibrium coverage. Contrary to expectations, the data exhibit no obvious trend in the surface coverage as a function of particle size, leading us to suspect that a secondary variable, such as differing hydrophobicities of the surfaces, influences the adsorption. This is presumably true for other dispersions showing anomalous dependence on particle radius as well.^{23,25}

For the densely covered surfaces, the layer thickness at full equilibrium coverage in 0.1 M NaCl detected by dynamic light scattering at $\theta = 90^\circ$ (Table 4) varies in qualitative accord with the surface coverage. The bare particles always yielded a polydispersity less than 0.05 and the size extracted from the initial slope of the correlation typically changed only 3% from 30° to 160° . The coated particles exhibited a slightly higher polydispersity (≈ 0.1) and typically less than an 8% change in the hydrodynamic size for the same range of scattering angles. So the measurements should be quite reliable.

The Daoud–Cotton model suggests correlating the layer thickness with surface coverage and particle radius by plotting $(L/R + 1)^{5/3}$ versus $L_c\sigma^{1/3}/R$, provided the solvent quality is constant. Figure 2 confirms that this yields a straight line with an intercept close to unity for our data. The positive slope (≈ 2.49) corresponds to $v/B \sim 15.4$ if $k = 1$. This is rather large but plausible for polyelectrolytes and certainly implies good solvent conditions, which justifies eq 3 for relating the number of segments in a blob to its size.

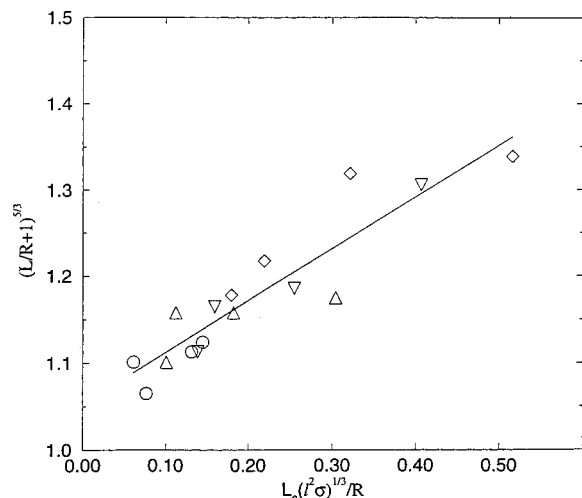


Figure 3. Data for four different PPO/PEO/PPO triblocks [F108 (circle), F88 (diamond), F68 (triangle up), and P105 (triangle down)] adsorbed on polystyrene latices plotted according to the Daoud–Cotton theory. A best-fit straight line for all the molecular weights yields an intercept of 1.05.

To test this interpretation further, we look to the data of Li et al.²³ for adsorption of poly(oxyethylene)/poly(oxypropylene)/poly(oxyethylene) triblocks with smaller molecular masses of the soluble blocks ($M_{\text{PEO}} = 1.6\text{--}5.7$ kg/mol) on polystyrene latices of similar sizes (69–272 nm). For these smaller L/R ratios, Figure 3 shows that the data for the four molecular weights and four particle sizes also correlates well when plotted according to eq 4, with an intercept close to unity and a slope of 0.6. The latter suggests $\nu/\beta \sim 0.22$ for PEO in water, which is quite plausible. This ability of the Daoud–Cotton model to correlate the effects of radius of curvature, chain length, and graft/adsorption density suggests generalizing the treatment by estimating the binary cluster integral (ν/β), which is the subject of our previous and following papers.^{15,48}

4.2. Effect of Ionic Strength. For the sparsely and densely covered particles, the influence of ionic strength on the thickness of the adsorbed layer for the 137 nm particles is depicted in Figure 4. The experiment effectively holds σ fixed and adjusts the ionic strength to swell or shrink the layer. The thickness of the sparse layer increases modestly from 27 nm at 1 M to 38 nm at 0.01 M NaCl, while the dense layer shows greater sensitivity. At 10^{-4} M the highly stretched chains extend to 195 ± 10 nm, which is very close to the contour length of 201 nm for the poly(styrenesulfonate) block and consistent with Pincus³⁰ prediction for the unsalted brush. With increasing salt concentration the brush shrinks, reaching about 42 nm at 1 M.

The curves in the figure are power law fits to the data ($L \sim C_s^{-m}$). The scaling exponent for the dense layer ($m = 0.17$) exceeds that for the sparse layer (0.08) but is lower than for densely coated, flat mica surfaces (0.21).¹² For complete coverage, the higher exponent for a flat plate (0.21) relative to the 137 nm particles (0.17) should represent the effect of curvature. With greater curvature, the volume available to segments at larger distances from the surface is higher, so the chains on a curved particle find more room to swell laterally. In contrast, the chains on a flat plate are confined by the neighboring segments equally at all distances from the surface and must swell outward, resulting in more pronounced changes in L with decreasing ionic strength

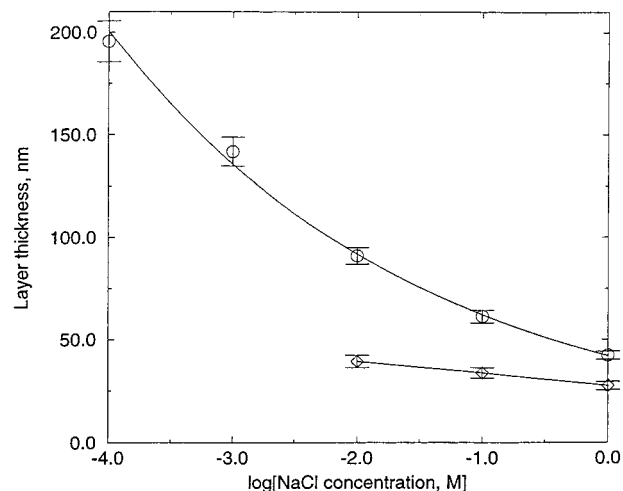


Figure 4. Thickness of adsorbed layer thickness as a function of added salt concentration for densely coated (circle) (adsorption at 0.1 M NaCl) and sparsely covered (diamond) (adsorption without added salt) particles of 137 nm diameter. The upper and lower curves represent power laws with $L \sim C_s^{-m}$ with $m = 0.17$ and 0.08, respectively.

or increasing excluded volume. All three experimental exponents compare poorly with the scaling predictions, $m = 0.33$, 0.50, and 0.67 (section 2.2), suggesting fundamental shortcomings in the models.

The power law exponent from the calculation by von Goeler and Muthukumar³⁶ depends on the dimensionless parameters $N^{1/2}k$ and $v_e N^{5/2}$ (eq 8). For the dense layer ($\Gamma = 1.9$ mg/m²) $v_e N^{5/2} = 3.1 \times 10^4$ and $0.5 < N^{1/2}k < 10$, which falls in the strong electrostatic screening regime where $L \sim C_s^{-1/3}$. This agrees with Pincus³⁰ but is contrary to the experimental data. For the sparsely covered surface ($\Gamma \approx 0.05$ mg/m²) $v_e N^{5/2} \sim 10^3$, for which von Goeler and Muthukumar predict a weaker dependence on ionic strength in qualitative accord with our observation.

For MT3 micelles, the hydrodynamic radius increases with decreasing salt concentration from 0.5 to 10^{-5} M (Figure 5), approaching a plateau below about 10^{-3} M. We interpret this as a limit in which the ionic strength in the brush is determined by the counterions, a subject that the following paper pursues.⁴⁸ The power law $L \sim C_s^{-0.11}$ fits the data for $C_s \geq 10^{-3}$ M, as shown in Figure 5.

We plot hydrodynamic dimensions of the polyelectrolyte blocks of MT3 and MT2 micelles,³⁹ our fully covered particles, and a homopolymer Na–poly(styrene sulfonate) of molecular mass 177 kg/mol, comparable to MT3,⁴⁹ as functions of salt concentration in Figure 6. All except the homopolymer can be viewed as grafted chains on a spherical interface. The exponents (m) for these and for MT3 adsorbed on mica in the surface forces apparatus¹² listed in Table 5 were calculated for $C_s \geq 10^{-3}$ M, as evident from the straight lines. Note that (1) the exponent for the homopolymer (0.07) is lowest, clearly illustrating the greater sensitivity of polymer chains crowded at the surface, (2) the larger aggregation number for MT2 (almost twice) compared to MT3 implies a larger core radius R_c via

$$R_c = \left(\frac{3pM_{\text{PtBS}}}{4\pi\rho_{\text{PtBS}}N_a} \right)^{1/3} \quad (13)$$

indicating that the salt sensitivity follows the core radii,

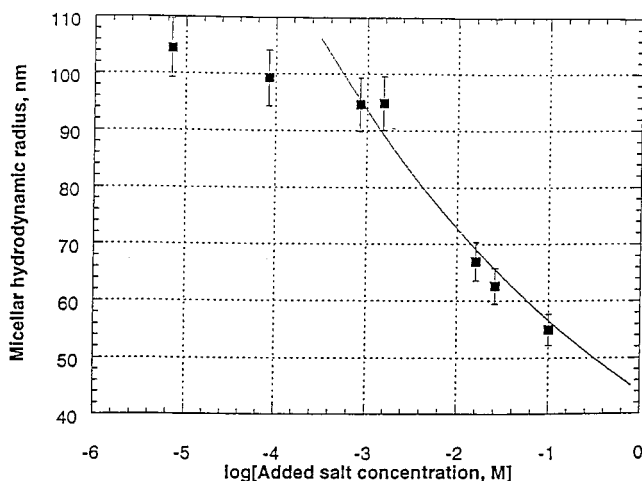


Figure 5. Hydrodynamic radius of MT3 as a function of added salt concentration with the curve corresponding to $L \sim C_s^{-0.11}$.

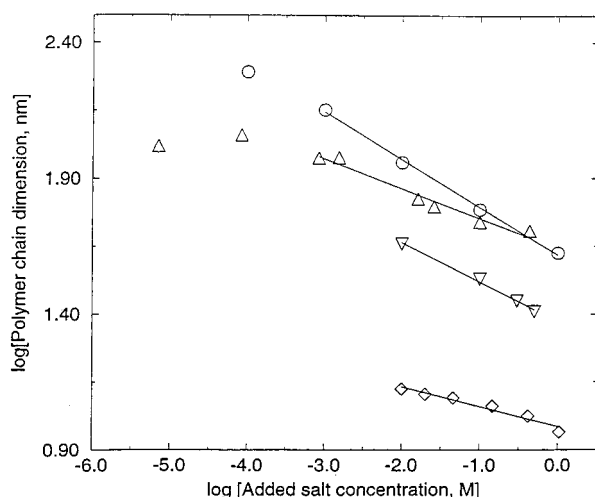


Figure 6. Layer thickness on 137 nm particles (circle), micellar radii [MT3 (triangle up) and MT2 (triangle down)], and homopolymer radius (diamond) (all hydrodynamic sizes) as a function of added salt concentration. The slopes for the best fit lines are -0.18 , -0.11 , -0.15 , and -0.07 , respectively.

Table 5. Scaling Exponent, Graft Density, and Interaction Strength for Polyelectrolyte Chains Extending from Spherical Interfaces in Order of Increasing Core Radius (and m)

system	m	σ	$v_e N^{5/2}$
MT3 micelles	0.11	0.15	6.0×10^5
MT2 micelles	0.14	0.18	1.8×10^4
MT3 on 137 nm polystyrene	0.17	7.7×10^{-3}	3.1×10^4
MT3 on mica (SFA)	0.21	1.4×10^{-2}	5.6×10^4

MT3 < MT2 < MT3 on 137 nm particle < MT3 on mica surface, and (3) the MT3 micelles exhibit higher values of $v_e N^{5/2}$ than the coated surfaces but are less sensitive to salt concentration, contrary to the predictions from von Goeler and Muthukumar for flat interfaces and further underlining the important coupling between curvature and ionic strength.

Two comments are in order here. First, a similar difference in sensitivity between tethered polymer chains and those in the bulk was observed⁵⁰ for diblock copolymers of poly((dimethylamino)ethyl methacrylate)/poly(*n*-butyl methacrylate) adsorbed on colloidal silica from a nonselective solvent. Second, the evident relationship between core radius and sensitivity to added salt is an oversimplification, since the surface density

is not held constant (Table 5). The differences between MT3 and MT2 in the micelles and MT3 on the 137 nm particle and the mica surface represent combined effects of decreased curvature and increased graft density.

5. A Simple Blob Model for Polyelectrolyte Brushes on Spheres

The exponents characterizing the sensitivity of the layer thickness to ionic strength for relatively flat layers compare poorly with the theoretical predictions (section 2.2.1). Here we show that the qualitative trends for both the flat and highly curved layers can be described reasonably faithfully with a slight modification of the blob models reviewed earlier.

If we follow the lead of Pincus in ignoring local chain stiffening but modify the excluded volume for interacting polyelectrolyte segments to the more realistic form derived by Odijk et al.,⁵¹ $v \sim P\kappa^{-1}$, then $v/\beta \sim C_s^{-1/2}$. Even though $k \leq 1$ for ionic strengths less than 10^{-2} M, the model for the excluded volume seems more appropriate.

The Daoud–Cotton model (eq 4) for a polymer brush now reduces to

$$\left(\frac{L}{R} + 1\right)^{5/3} = 1 + k \frac{L_c}{R} \left(\frac{l\sigma}{\kappa}\right)^{1/3} \quad (14)$$

For $R \rightarrow \infty$,

$$L_\infty \approx L_c \left(\frac{l\sigma}{\kappa}\right)^{1/3} \quad (15)$$

which means $L_\infty \sim C_s^{-1/6}$. This prediction closely resembles the trend for our fully coated particle (-0.17) but is weaker than that for the flat mica surface (-0.21) of Watanabe et al.¹² In the $R \rightarrow 0$ limit, the model reduces to

$$L_0 \approx L_c^{3/5} R^{2/5} \left(\frac{l\sigma}{\kappa}\right)^{1/5} \quad (16)$$

which means $L_0 \sim C_s^{-1/10}$. This result matches closely the observed slope (0.11) for MT3 but is somewhat weaker than for MT2 (0.145). As discussed earlier, MT3 has a smaller core radius than MT2 and might be closer to the $R \rightarrow 0$ limit. Nonetheless, the predictions are closer to the experimental values in both limits than all previous theories for highly charged, salted polyelectrolyte brushes.^{30,32,34,36}

6. Conclusions

A polyelectrolyte diblock was adsorbed on colloidal polystyrene by carefully tuning the electrostatics. Measurements of the adsorbed amount and layer thickness lead to several conclusions on the effect of curvature and ionic strength:

(1) Uncontrolled aspects of surface chemistry produce uncorrelated variations in surface coverage as a function of curvature.

(2) Variations of layer thickness with curvature and surface coverage are well understood through the Daoud–Cotton theory.

(3) Curvature strongly influences the sensitivity of a polyelectrolyte brush to added salt.

(4) A simple model for electrostatic interactions in highly charged polyelectrolyte brushes along the lines of Pincus and Argiller and Tirrell accounts for the sensitivity of layer thickness to added salt for flat and highly curved brushes better than previous theories.

(5) Coupled curvature and ionic effects, along with the success of the Daoud–Cotton theory in describing the role of curvature, motivate the more detailed electrostatic blob model in the following paper.⁴⁸

Acknowledgment. The authors would like to thank Patrick Guenoun, Guy Chavauteau, Matthew Tirrell, and Stan Lam for many insightful discussions. Elf Aquitaine, Elf Atochem, and the National Science Foundation through NSF/CTS-9107025 and the MR-SEC/DMR9400362 are gratefully acknowledged for their financial support.

References and Notes

- (1) Marques, C.; Joanny J. F.; Leibler, L. *Macromolecules* **1988**, *21*, 1051.
- (2) Marques, C.; Joanny J. F. *Macromolecules* **1989**, *22*, 1454.
- (3) Parsonage, E.; Tirrell, M.; Watanabe, H.; Nuzzo, R.G. *Macromolecules* **1991**, *24*, 1987.
- (4) Patel, S. S.; Tirrell, M.; Hadzioannou, G. *Colloids Surf.* **1988**, *31*, 157.
- (5) Munch, M. R.; Gast, A. P. *Macromolecules* **1988**, *21*, 1360.
- (6) Taunton, H. J.; Toprakcioglu, C.; Fetters, L. J.; Klein, J. *Macromolecules* **1990**, *23*, 571.
- (7) Takahashi, A.; Kawaguchi, M. *Adv. Polym. Sci.* **1982**, *46*, 46.
- (8) Cohen Stuart, M. A.; Cosgrove, T.; Vincent, B. *Adv. Colloid Interface Sci.* **1986**, *24*, 143.
- (9) Kawaguchi, M.; Takahashi, A. *Adv. Colloid Interface Sci.* **1992**, *37*, 219.
- (10) Fixman, M.; Skolnick J. *Macromolecules* **1978**, *11*, 863.
- (11) Fixman, M. *J. Chem. Phys.* **1990**, *92*, 6283.
- (12) Watanabe, H.; Patel, S. S.; Argiller, J. F.; Parsonage, E.E.; Mays J.; Dan Brandon, N.; Tirrell, M. *Mater. Res. Soc. Symp. Proc.* **1992**, *249*, 255.
- (13) Amiel, C.; Sikka, M.; Schneider, W.; Tirrell, M.; Mays, J. *Macromolecules* **1995**, *28*, 3125.
- (14) Daoud, M.; Cotton, J. P. *J. Phys. (Paris)* **1982**, *43*, 531.
- (15) Biver, C.; Hariharan, R.; Mays, J.; Russel, W. B. *Macromolecules* **1997**, *30*, 1787.
- (16) Hariharan, R. Ph.D. dissertation, Princeton University, 1996.
- (17) Halperin, A. *Macromolecules* **1987**, *20*, 2943.
- (18) Ligoure, C.; Leibler, L. *Macromolecules* **1990**, *23*, 5044.
- (19) Qiu, X.; Wang, Z. *J. Colloid Interface Sci.* **1994**, *167*, 294.
- (20) Garvey, M. J.; Tadros, Th. F. *Proc. Int. Conf. Surface Active Agents*, 6th **1973**.
- (21) Garvey, M. J.; Tadros, Th. F.; Vincent, B. *J. Colloid Interface Sci.* **1974**, *49*, 57.
- (22) Baker, J. A.; Pearson, R. A.; Berg, J. C. *Langmuir* **1989**, *5*, 339.
- (23) Li, J.; Caldwell, K. D.; Rapoport, N. *Langmuir* **1994**, *10*, 4475.
- (24) Singh, N.; Karim, A.; Bates, F. S.; Tirrell, M.; Furusawa, K. *Macromolecules* **1994**, *27*, 2586.
- (25) Merrington A.; Yang, Z.; Meier, D. J. *ACS Colloid Surf. Symp.*, 68th **1994**.
- (26) Miklavic, S. J.; Marcelja, S. *J. Phys. Chem.* **1988**, *93*, 6718.
- (27) Misra, S.; Varanasi, S.; Varanasi, P. P. *Macromolecules* **1989**, *22*, 4173.
- (28) Milner, S. T.; Witten, T. A.; Cates, M. E. *Macromolecules* **1989**, *22*, 853.
- (29) Alexander, S. *J. Phys. Paris* **1977**, *38*, 983.
- (30) Pincus, P. *Macromolecules* **1991**, *24*, 2912.
- (31) Pincus, P.; Witten, T. *Europhys. Lett.* **1987**, *3*, 315.
- (32) Argiller, J. F.; Tirrell, M. *Theor. Chim. Acta* **1992**, *82*, 343.
- (33) Zhulina, E. B.; Borisov, O. V.; Birshtein, T. M. *J. Phys. II Fr.* **1992**, *2*, 63.
- (34) Dan, N.; Tirrell, M. *Macromolecules* **1993**, *26*, 4310.
- (35) Davis, R. M.; Russel, W. B. *J. Polym. Sci., Polym. Phys. Ed.* **1996**, *24*, 511.
- (36) von Goeler, F.; Muthukumar, M. *Macromolecules* **1995**, *28*, 6608.
- (37) Pefferkorn, E.; Schmitt, A.; Varoqui, R. *Biopolymers* **1988**, *21*, 1451.
- (38) Valint, P. L.; Bock, J. *Macromolecules* **1988**, *21*, 175.
- (39) Guenoun, P.; Davis, H. T.; Tirrell, M.; Mays, J. W. *Macromolecules* **1996**, *29*, 3965.
- (40) Mir, Y.; Auroy, P.; Auvray, L. *Phys. Rev. Lett.* **1995**, *75* (15), 2863.
- (41) Guenoun, P.; Schlachli, A.; Sentenac, D.; Mays, J. W.; Benattar, J. *J. Phys. Rev. Lett.* **1995**, *74*, 3628.
- (42) Russel, W. B.; Saville, D. A.; Schowalter, W. R. *Colloidal Dispersions*; Cambridge University Press: Cambridge, U.K., 1989.
- (43) Pusey, P. N. In *Photon Correlation and Light Beating Spectroscopy*; Cummins, H. Z., Pike, E. R., Eds.; Plenum Press: New York, 1974.
- (44) Garvey, M. J.; Tadros, Th. T.; Vincent, B. *J. Colloid Interface Sci.* **1976**, *55*, 440.
- (45) Huglin, M. B. *Light Scattering from Polymer Solutions*; Academic Press: New York, 1972.
- (46) Guenoun, P.; Lipsky, S.; Mays, J. W.; Tirrell, M. *Langmuir* **1996**, *12*, 1425.
- (47) Wittmer, J.; Joanny, J. F. *Macromolecules* **1993**, *26*, 2691.
- (48) Hariharan, R.; Biver, C.; Russel, W. B. *Macromolecules* **1998**, *31*, 7514.
- (49) Wang, L.; Yu, H. *Macromolecules* **1988**, *21*, 3498.
- (50) Hariharan, R.; Russel, W. B. *Langmuir*, in press.
- (51) Odijk, T.; Houwaart, A. C. *J. Polym. Sci., Polym. Phys.* **1978**, *16*, 627.

MA971818G